Published in final edited form as:
Genes Chromosomes Cancer. 2013 November ; 52(11): 1017–1029. doi:10.1002/gcc.22097.

Common Chromosome Fragile Sites in Human and Murine Epithelial Cells and *FHIT/FRA3B* Loss-Induced Global Genome Instability

Seyed Ali Hosseini[1], **Susan Horton**[2], **Joshua C. Saldivar**[1], **Satoshi Miuma**[1], **Martha R. Stampfer**[3], **Nyla A. Heerema**[2], and **Kay Huebner**[1,*]

[1]Department of Molecular Virology, Immunology and Medical Genetics, The Ohio State University Wexner Medical Center, Columbus, OH

[2]Department of Pathology, The Ohio State University Wexner Medical Center, Columbus, OH

[3]Life Sciences Division, Lawrence Berkeley National Laboratory, Berkeley, CA

Abstract

Chromosomal positions of common fragile sites differ in lymphoblasts and fibroblasts, with positions dependent on the epigenetically determined density of replication origins at these loci. Because rearrangement of fragile loci and associated loss of fragile gene products are hallmarks of cancers, we aimed to map common fragile sites in epithelial cells, from which most cancers derive. Among the five most frequently activated sites in human epithelial cells were chromosome bands 2q33 and Xq22.1, which are not among top fragile sites identified in lymphoblasts or fibroblasts. *FRA16D* at 16q23 was among the top three fragile sites in the human epithelial cells examined, as it is in lymphoblasts and fibroblasts, while *FRA3B* at 3p14.2, the top fragile locus in lymphoblasts, was not fragile in most epithelial cell lines tested. Epithelial cells exhibited varying hierarchies of fragile sites; some frequent epithelial cell fragile sites are apparently not frequently altered in epithelial cancers and sites that are frequently deleted in epithelial cancers are not necessarily among the most fragile. Since we have reported that loss of expression of the *FRA3B*-encoded FHIT protein causes increased replication stress-induced DNA damage, we also examined the effect of FHIT-deficiency on markers of genome instability in epithelial cells. FHIT-deficient cells exhibited increases in fragile breaks and in γH2AX and 53BP1 foci in G1 phase cells, confirming in epithelial cells that the *FHIT* gene and encompassing *FRA3B*, is a “caretaker gene” necessary for maintenance of genome stability.

INTRODUCTION

Almost since their discovery common fragile sites (CFSs) have been the subject of debate concerning the cause of sensitivity to DNA damage at these loci and the biological

*Correspondence to: Kay Huebner, Department of Molecular Virology, Immunology and Medical Genetics, The Ohio State University Wexner Medical Center, The Biomedical Research Tower, rm 916. 460 W 12th Ave., Columbus, OH 43210, USA. kay.huebner@osumc.edu.

Additional Supporting Information may be found in the online version of this article.

consequences of damage to genes encompassing CFSs. Letessier et al. (2011) have recently reported that the fragility at *FRA3B*, encompassed by the *FHIT* gene, the most active CFS in human lymphoblasts, does not rely on fork slowing or stalling but rather on scarcity of replication initiation events within the locus. In lymphoblasts, but not in fibroblasts, initiation events are absent from the central fragile region of *FRA3B*, so that replication of this large region within the *FHIT* gene must be completed by convergence of flanking replication forks. Fibroblasts did not exhibit the fragility at *FRA3B* observed in the many lymphoblast cells tested over the years since CFS discovery. Nor was *FRA16D*, the second most active lymphoblast CFS, particularly fragile in fibroblasts, confirming earlier reports of tissue specificity of CFSs (Djalali et al., 1987; Murano et al., 1989a,b). An important conclusion of this study was that CFSs correspond to the initiation poor regions that finish replication latest in a given cell type (Huebner, 2011; Letessier et al., 2011; Debatisse et al., 2012).

The two genes *FHIT* and *WWOX*, at *FRA3B* and *FRA16D*, are among the most frequently altered by DNA deletion in precancerous and cancerous cells of epithelial origin (Sozzi et al., 1998; Mori et al., 2000; Bartkova et al., 2005; Gorgoulis et al., 2005) presumably due to exposure of tissues of these organs to replicative stress-causing agents. It has been argued that damage to genes at specific CFSs and loss of expression of the gene products contributes to selective growth of the precancers or cancers (Ohta et al., 1996; Huebner and Croce, 2001; Saldivar et al., 2012); counter arguments claim that the frequent deletions within these fragile loci means that loss of their expression occurs as unselected passenger events in cancers (Bignell et al., 2010; Negrini et al., 2010) and that loss of these genes does not contribute to the clonal expansion of precancerous cells. But what if these regions are not among the most fragile loci in epithelia? If not, this finding would support the argument that their very frequent deletion in precancers and cancers of epithelial tissues has contributed to progressive growth of the lesions. To initiate answers this question, we have mapped CFSs in human and murine cells of epithelial origin, in comparison to lymphoblasts.

In addition, we have previously shown, in normal, transformed, and cancer-derived cell lines, that FHIT depletion causes increased replication stress-induced DNA double-strand breaks. Depletion of FHIT protein did not activate the DNA damage response nor cause cell cycle arrest, allowing continued cell proliferation and ongoing chromosomal instability. Furthermore, cells established from *Fhit* knockout tissue showed rapid immortalization and selection of DNA deletions and amplifications, suggesting that FHIT loss-induced genome instability facilitates transformation (Saldivar et al., 2012; Miuma et al., unpublished data). Thus, we have also examined the effects of loss of expression of the *FHIT/FRA3B* locus on global genome stability in epithelial cells.

Thus, the goals of the current study were two-fold: (1) to determine the hierarchy of CFSs in epithelial tissue-derived cells; and (2) to confirm findings that *FHIT* protein deficiency increases expression of markers of global genome instability (Saldivar et al., 2012), increased CFS activation, and increased γH2AX and 53BP1 localization at nuclear foci, in epithelial cells. We have defined genomic locations of CFSs in established epithelial cell lines derived from mouse and human tissues to determine if they differ from those of lymphoblasts, are sites that are frequently broken or mutated in epithelial cancer cells, and if

loss of FHIT protein expression causes increased genome instability in such cells. Knowledge of the most active CFSs of epithelial cells may contribute to understanding of the earliest genetic changes that occur in epithelial cells on the path to cancer development.

MATERIALS AND METHODS

Cell Lines and Reagents

Fhit+/+ and *Fhit*−/− mouse kidney epithelial cells from C57B1/B6 background mice were cultured in MEM with 10% FBS and 100 μg/ml gentamicin. The human mammary epithelial cell lines MCF10A (Soule et al., 1990) and 184A1 cells (Stampfer and Bartley, 1985) were, respectively, grown in F12/DMEM and HuMEC medium with 25 mg Bovine Pituitary Extract and supplements (Gibco/Invitrogen, Grand Island, NY cat#12753-018, 12754-016, 13028-014) (Keller et al., 2012); SV40 T antigen transformed BEAS2B lung epithelial cells and GM1500 lymphoblastoid cells from the Coriell Cell Repository (Camden, NJ) were grown in DMEM and RPMI, respectively, with addition of 10% FBS and gentamicin antibiotic. HCT116 colon cancer cells were grown in RPMI-1640 with addition of 10% FBS and gentamicin antibiotic.

shRNA Silencing

Short hairpin RNAs (shRNAs) can induce sequence-specific gene silencing in mammalian cells (Paddison et al., 2002). A lentiviral construct containing a puromycin resistance gene as well as sh*FHIT* insert was used to target both alleles of *FHIT* in the MCF10A cells. MCF10A cells (60–80% confluent) were infected with lentiviral shRNAs targeting human *FHIT* or a nonspecific control shRNA (Santa Cruz Biotechnology, Dallas, TX) using the manufacturer's recommended protocol. For each 60 mm dish, 1 mg of shRNAs and 6 μl of Lipofectamine 2000 (Invitrogen) were diluted in Opti-MEM (Gibco) and incubated for 45 min. Cells were washed in Opti-MEM, overlaid with the shRNA/Lipofectamine solution, and incubated overnight at 37°C. Verification of shRNA knockdown (KD) of *FHIT* expression by western blot was performed after selection in 2 μg/ml puromycin.

Immunofluorescence Assays

Cells were grown on eight-chamber slides, fixed with 4% paraformaldehyde, permeabilized with ice-cold 70% ethanol, and blocked in 1% BSA. Primary antisera, rabbit anti-γH2AX, or rabbit anti-53BP1 (Cell Signaling Technologies, Danvers, MA), diluted 1:200, were added and cells incubated with antisera overnight at 4°C. Slides were washed 3 × 10 min in PBS, and secondary antisera (AlexaFluor 488 or 594—conjugated donkey anti-rabbit IgG or anti-mouse IgG, 1:500, Molecular Probes, Grand Island, NY) were added and incubated for 1 hr at room temperature. Slides were washed and mounted using Fluoro-Gel II—with DAPI Images were acquired with an Olympus FV1000 confocal microscope and analyzed using Image J software. For all immunofluorescence assays 100 cells were analyzed in each of three independent experiments.

Western Blot Analysis

Cells were lysed with RIPA buffer supplemented with Protease Cocktail Inhibitors (Thermo Scientific, Pittsburgh, PA), and immunoblot analyses were performed as described

previously (Saldivar et al., 2012). Proteins were separated by SDS gel electrophoresis, transferred to nylon membranes, and immunoblotted with antisera against human FHIT, GAPDH, and human TK1 (AbD Serotec, Oxford, UK).

Preparation of Metaphase Spreads and Fragile Site Analysis

Fragile sites were induced by exposure of cells to 0.4 μM aphidicolin (Aph) for 18 hr before harvest. *Fhit*+/+ or *Fhit*−/− mouse kidney cells at the 8th subculture, MCF10A1 shCtrl and sh*FHIT*, 184A1, BEAS2B, HCT116, and GM1500 cells were harvested for chromosome preparation by standard conditions after a 2 hr colcemid treatment (0.01 μg/ml) to block cells in mitosis. Cells were trypsinized, pelleted, and resuspended in 0.075 M KCl hypotonic solution for 15 min at 37°C. Cells were fixed in methanol/acetic acid (3:1), dropped on glass slides, and allowed to air dry. G-banding was performed for identification of fragile sites (Seabright, 1971) at specific human and mouse chromosome bands. Chromosomes were analyzed using a Zeiss Axioskop Widefield LM at 100× magnification. Twenty to 44 metaphases were analyzed for assessment of numbers and positions of CFSs in these cells, as noted in the legend to Table 1.

Copy Number Variation Analysis

DNA was isolated using a DNeasy Kit (Qiagen, cat# 69506, Germantown, MD). High-resolution copy number analysis (CNV) was performed in the Nationwide Childrens' Hospital Research Institute core facility, using the Agilent Human Genome CGH Microarray 4x180K (Santa Clara, CA).

Statistical Analysis

For boxplots, the bottom and top of the box correspond to the 25th and 75th percentiles, respectively, and whiskers represent data points within 1.5 × IQR (interquartile range). Two-sided *t*-tests were used to determine significance for data with a normal distribution and equal variances. Non-parametric data were analyzed using the Mann-Whitney rank sum test for single comparisons or using the Kruskal-Wallis test for multiple comparisons. *P* values <0.05 were considered to indicate statistical significance.

RESULTS

CFSs in Cells of Human and Murine Epithelial Origin

We determined the most frequently activated fragile sites in epithelial cells, using cell lines that would grow for numerous subcultures, so that we could also examine the effect on fragility and genome instability in these cells when the *FHIT* gene was silenced. Two nonmalignant immortal breast cell lines were used: MCF10A breast epithelial cells immortalized after explanting fibrocystic tissue from a subcutaneous mastectomy surgery (Soule et al., 1990); the 184A1 line derived from normal reduction mammoplasty tissue and immortalized following exposure to a chemical carcinogen (Stampfer and Bartley, 1985); both cell lines are near diploid, estrogen receptor and p16/CDKN1A negative. As shown in the Figure 1 graph in the upper panel, for the MCF10A breast epithelial cell line, the CFSs identified were, in order of frequency: 16q23 (*FRA16D/WWOX*) > 2q33 (*FRA2I*), 5q15 (*FRA5D*) > 1q23, 2q21, 12q22, and Xq22 (representative karyotype in Supporting

Information Fig. S1). For 184A1 cells the CFSs were 16q23 > 3q26.2, Xq22, 12q22, 14q24.3 > 7q11.2, and Xp21.2 (not shown graphically, see Table 1 for summary); for the HCT115 colon carcinoma-derived cells the top four CFSs were 16q23, 2q33, 4q21.3, Xp22.3, and Xq22.1, respectively (Table 1); and for comparison with lymphoblastoid cells, the CFSs observed for GM1500 were: 16q23 > 3p14.2 (*FRA3B/FHIT*) > 4q35 > 8q22, Xp22.1 > 6q25.1, 1p22, and 9q12 (data for all cells examined by us in comparison with lymphoblasts and fibroblasts examined by others are summarized in Table 1).

BEAS2B cells, established by transformation of normal human lung bronchial epithelial cells by SV40 T antigen, exhibit three cytogenetically distinct subclones, two of which are near-tetraploid. In BEAS2B cells the most active CFSs were 3p14.2 > 2q33 > 16q23 > Xq22.1 > 13q32 > 1p31.2, 7q31.2, and 7q11.2 (Fig. 1 lower panel, Table 1 for comparative summary), which varies somewhat from active CFSs in lymphoblasts, fibroblasts and the other epithelial cells we examined.

Origins of Replication at CFSs of Epithelial Cells

A genome-scale approach—Repli Seq—has been developed (Hansen et al., 2010) to map temporally ordered replicating DNA using massively parallel sequencing and applied to study regional variation in human DNA replication time across multiple human cell types, providing high-resolution DNA replication patterns relative to cell-cycle time and genomic position; the investigators have shown that different cell types exhibit characteristic replication signatures with plasticity in regional replication time patterns over much of the human genome (Consortium et al., 2011, 2012). This Repli-seq database was used previously to show the association of paucity of replication origins and late timing of replication completion with fragility of *FRA3B* and *FRA16D* in lymphoblasts, while fibroblasts showed increased replication origins and earlier completion of replication in these regions (Letessier et al., 2011). We have used the Repli-seq database to compare density of replication origins and replication timing in three CFSs, *FRA3B* (3p14.2), *FRA16D* (16q23) and *FRA2I* (2q33) in human lymphoblast and epithelial cells (Fig. 2). In Figure 2, right panel, are the Repli-seq drawings for the replication origins and S-phase replication timing for a lymphoblast line in which both *FRA3B* and *FRA16D* show no replication origins within the fragile regions (bracketed by the vertical lines within the drawing). We know that *FRA3B* and *FRA16D* are highly fragile in lymphoblasts and would predict that *FRA2I* replication would be completed late in S phase in lymphoblasts with contribution of the S4 activated replication origin. The Repli-seq data reproduced in Figure 2, left panel, illustrates the replication programs of the same three regions in the epithelial NHEK cell (normal human epidermal keratinocytes). The replication program for *FRA16D* is compatible with fragility while *FRA3B* would be predicted not to be fragile in this epithelial cell, in accord with our data for the MCF10A and 184A1 cells. The replication program for FRA2I is also compatible with fragility in epithelial cells.

Effect of Loss of FHIT Protein Expression on CFS Activity in Epithelial Cells

We had previously observed that fibroblasts derived from *Fhit* knockout mice showed a two-fold increase in average numbers of gaps per chromosome (Turner et al., 2002) and have now shown that loss of FHIT protein expression can lead to global genome instability

(Saldivar et al., 2012). Thus, we have examined the effect of FHIT protein expression deficiency on frequency and hierarchy of CFS activation in epithelial cells.

Cytogenetics of noncancerous mouse kidney (MK) epithelia-derived cell lines established from explants of baby mouse kidney of a wild-type (WT) *Fhit*+/+ and *Fhit*−/− (KO) mouse (Saldivar et al., 2012; Miuma et al., unpublished data) were examined with and without Aph treatment. In comparisons of the locations and frequencies of activation of CFSs in MK cells with and without Aph treatment (Figs. 3 and 4), we observed approximately twofold increases in the frequencies of fragile breaks in the *Fhit*−/− cells. Figure 4 (upper panel) shows the distribution and frequencies of activation of the fragile sites in +/+ versus −/− MK cells. Note that the mouse band 8E1 corresponds to *FRA16D/WWOX* (Krummel et al., 2002) in human and band 14A2 is equivalent to human *FRA3B/FHIT*. The hierarchy of frequent CFSs differs slightly in the *Fhit*−/− versus +/+ MK cells, though we do not know if the difference is *Fhit*-specific. Moreover, MK Fhit silenced cells showed substantially increased levels of chromosomal aneuploidy, including chromosome losses and gains (not shown).

We also examined the frequency of CFS activation after treatment with Aph in the immortal non-cancerous MCF10A cells after FHIT protein expression KD by shRNA. MCF10A cells were transfected with *FHIT*-specific shRNA to study the effect of FHIT protein KD on CFSs in epithelial cells (see Supporting Information Fig. S2B for illustration of FHIT protein KD by shRNA); we found that there were variations in the frequency of activation of specific CFSs in the FHIT positive and deficient MCF10A cells after 18 hr treatment with 0.4 μm Aph (Fig. 4, lower panel). Karyotypic analysis revealed that the FHIT KD cells exhibited an approximately twofold increase in frequency of gaps and breaks compared with FHIT-positive cells (breaks per chromosome in MCF10A compared with MCF10A/FHIT KD, 0.027/0.058).

Additional Markers of FHIT Loss-Induced Genome Instability in Epithelial Cells

Sister chromatid exchanges (SCEs) can be induced by various genotoxic treatments (Hagmar et al., 1998; Sonoda et al., 1999), suggesting that SCEs reflect a DNA repair process and a link between SCE and DNA replication. CFSs are hot-spots for SCE formation, which are formed by the action of homologous recombination during replication (Sonoda et al., 1999). To measure the frequency of SCEs in FHIT-deficient cells, *Fhit*−/− and *Fhit*+/+ MK cells were labeled with BrdU for two full cell cycles (40–48 hr). The frequency of spontaneous SCEs in +/+ MK cells was 0.27 exchanges per chromosome (Figs. 5A and 5B), while MK *Fhit*−/− cells showed 0.48 exchanges per chromosome, illustrating that loss of FHIT protein in epithelial cells is sufficient to cause a dramatic increase in chromosomal instability, even in the absence of exogenous genotoxic agents.

To address the mechanism for increased chromosomal instability in these FHIT-deficient cells, we hypothesized that it is due to DSBs during DNA replication, as shown previously for several cell types (Saldivar et al., 2012). After FHIT KD in MCF10A cells by sh*FHIT* lentiviral infection, western blot analysis revealed a decrease in the level of FHIT and thymidine kinase 1 (TK1, Supporting Information Fig. S2B) which would cause pyrimidine pool disequilibrium and contribute to genome instability of FHIT-deficient epithelial cells. There was also an increase in the basal levels of phospho-53BP1 and γH2AX, markers of

DNA breaks, with an average of 26% of 53BP1 positive sh*FHIT* cells versus 15% positive shCtrl cells (Figs. 6A and 6B) and for γH2AX foci 60% positive sh*FHIT* versus 37% positive shCtrl cells (Figs. 6C and 6D), suggesting that MCF10A FHIT KD cells are not only more sensitive to genotoxic agents but are also undergoing spontaneous chromosomal alterations, supporting our proposal that FHIT-deficient cells accumulate genetic lesions.

To complement the study of markers of genome instability in MCF10A cells after FHIT KD, we have maintained sh*FHIT* silenced MCF10A cells for 30 days, prepared DNA of MCF10A control and MCF10A FHIT KD cells and have assessed chromosome copy number alterations in the MCF10A KD DNA versus MCF10A control DNA by Comparative Genome Hybridization Microarray analysis. In this comparison, we observed copy number gains and losses specific for FHIT KD as listed in Table 2, which also lists genes that are included in the lost and gained loci. It is interesting that even though the MCF10A cells are immortal cells with numerous previous genetic alterations (Soule et al., 1990; Worsham et al., 2006; Kadota et al., 2010), loss of FHIT expression even for only 30 days, induces additional genome instability.

Genetically unstable cells are known to exhibit abnormal nuclear structures, such as micronuclei (Iarmarcovai et al., 2008). To characterize further the unstable phenotype of the FHIT KD cells, we assessed numbers of micronuclei. Cells were stained with DAPI to visualize chromatin using fluorescence microscopy and subsequently scored for the presence of this type of nuclear alteration. Micronucleus formation in MCF10A cells carrying sh*FHIT* versus shCtrl was increased >2-fold, with 12% of FHIT-silenced cells *vs* 5.6% of control cells showing micronuclei (Figs. 5C and 5D), further supporting the finding that reduction in FHIT protein expression in established epithelial cell lines leads to the development of chromosomal instability.

DISCUSSION

CFSs in Epithelial Cells

It is of interest that 16q23 (*FRA16D/WWOX*) shows the greatest fragility in all the epithelial cell lines except BEAS2B where it is the second most active site. This CFS is also in the top three in lymphoblast and fibroblast cell lines, and the encompassing gene, WWOX, is reduced in expression in many types of cancer, including breast cancer (Guler et al., 2004). It is possible that the in vitro growth of the mammary gland cells involved a selective process that led to expansion of clones with the CFS characteristics observed, though it is generally observed that CFSs in primary, cultured, and even EBV-transformed lymphoblasts are similar, so there has so far not been a suggestion that the hierarchy of CFSs in a particular cell type is influenced by selective growth conditions. Likewise it is interesting that 3p14.2 (*FRA3B/FHIT*) was most fragile in the lung epithelial cell since FHIT protein is very frequently lost or reduced in lung and other preneoplasias (Sozzi et al., 1998; Mori et al., 2000; Wistuba et al., 2000; Bartkova et al., 2005; Gorgoulis et al., 2005), likely influenced by sensitivity of the site to replication stress, and indeed FHIT expression is lost in the BEAS2B cells (Supporting Information Fig. S2A). This suggests that the transformation of the bronchial epithelial parental cells by SV40 T antigen involved selective growth of cell clones with *FRA3B* fragility and loss of FHIT expression. On the

other hand, 2q33 (*FRA2I*), in the top three CFSs in four of the epithelial cell lines examined, is not a frequently altered CFS in lymphoblasts and thus has not been considered an important CFS previously, though this locus and others identified as CFSs in these epithelial cells may encompass genes that have been reported to be cancer-associated as summarized in Table 3. In all epithelial cells examined at least two CFSs in the top five are the same. Table 3 lists possible tumor suppressor genes that were reportedly deleted in cancer cell lines and are near or possibly within some of the epithelial cell CFSs observed in this study.

In comparing the murine MK−/− and +/+ cells, three of the five most active Aph-induced CFSs are the same though the hierarchy of frequency within the top five differs. These are cell lines at early tissue culture passage, p8, but may have been selected for expansion of specific clones. If so, it is interesting that the *Fra14A2/Fhit* locus is among the CFSs observed in the MK+/+ but not in the −/− cells where its loss could not provide a selective advantage due to knockout of its expression. The murine equivalent (8E1) of the human 16q23/*FRA16D/WWOX* locus is among the top four CFSs (as in human epithelial cells) in the MK cells and is the most active in the MK−/− cells. Also of interest, the murine equivalent (1C2) of the human 2q33/*FRA2I* locus is among the top three CFSs in the MK−/− cells; these results may suggest that growth in tissue culture has influenced the growth of variant clones but that there is overall similarity in selection in the murine and human epithelial cells, with variations perhaps dependent on combinations of tissue of origin and transforming influence (loss of *FHIT*, loss of *CDKN2A*, gain of SV40 T, with concomitant inactivation of *RB1* and *TP53* by T antigen).

Would some of the variation in Aph-induced fragile site frequency and hierarchy among the epithelial cells disappear if we studied normal proliferative cells from the various epithelial organs rather than immortalized lines? The answer is not readily apparent although there is near universal agreement that the top two CFSs in lymphoblasts, whether primary or EBV transformed, are *FRA3B* and *FRA16D* and *FRAXB*/Xp22 is always in the top five. We note that we also assayed for Aph-induced CFSs in HCT116 colon cancer cells, a cancer cell line that expresses abundant FHIT protein (Supporting Information Fig. S2A). For this cell line, too, 16q23/*FRA16D/WWOX* and *FRA2I*/2q33 are the top CFSs.

Because a top CFS of each epithelial cell line, regardless of the altered gene (sh*FHIT*, *CDKN2A* mutant, and SV40 T), is *FRA16D*, there is no indication of a large influence of a specific transforming agent, just as there is not for the EBV-transformed lymphoblasts.

An interesting observation in MCF10A cells following FHIT KD was that the twofold increase in chromosome breaks/gaps included induction of several novel fragile loci including 7q22, 9p22, 1q44, and 2q23. What these loci have in common that make them particularly sensitive to FHIT absence is unknown. Perhaps their expression is a consequence of the reduced replication fork velocity and increased replication fork stalling and collapse in FHIT-deficient cells.

Repli-Seq Data for Epithelial Cells vs Lymphoblasts and Fibroblasts

It is also of interest that the Repli-seq data for three of our top epithelial fragile regions support the model of fragility dependent on placement of DNA replication origins in cells

derived from specific tissues (Letessier et al., 2011). As noted in the results section, the *FRA3B* locus of NHEK epithelial cells shows Repli-seq data that would suggest it is less fragile in these cells than in lymphoblasts as we have observed in the cytogenetics experiments, while *FRA16D* shows very similar distributions of replication origins in the epithelial and lymphoblast cells from the Repli-seq database. *FRA2I/2q33* should be more fragile in epithelial cells and less fragile in lymphoblast cells, showing concordance between our findings and the Repli-seq examples shown in Figure 2.

In summary, epithelial cells show differences and similarities in active CFSs when compared with lymphoblasts, with *FRA16D* among the most active in both and thus among the most sensitive to replication stress in cells of epithelial and lymphoblast origin. Expression of the WWOX protein is very frequently reduced or absent in human solid tumors, particularly breast cancers (Guler et al., 2004). Breast cancer cells also show reduced or absent expression of FHIT in >60% of cancers and yet the *FRA3B/FHIT* locus is apparently not fragile in breast epithelial cells. This finding may lend some weight to the idea that loss of FHIT expression is selected for during breast cancer initiation or progression.

Genome Instability in FHIT-Deficient Epithelial Cells

We have previously shown (Saldivar et al., 2012) that loss of expression of FHIT leads to genomic instability in mouse embryo fibroblasts, established mouse kidney cells, and human embryonic kidney cells transformed by Adenovirus 5 T antigen (293 cells after si*FHIT*), but had not carried out extensive studies of cells derived from non cancerous epithelia of various organs, particularly in combination with cytogenetic studies of CFS activation. Since most solid human cancers, carcinomas and adenocarcinomas, derive from the epithelia of major internal organs, our aim was to examine genome instability and its link to fragile site activation in non-malignant epithelia-derived cell lines. In each experiment in which FHIT expression was reduced, we observed increasing levels of instability whether measured by activity of CFSs or by markers such as SCE, γH2AX, and 53BP1 foci, or micronucleus frequency. Even in cells in which FHIT was absent or reduced, such as BEAS2B, the average number of CFS breaks per chromosome was more than fivefold greater than in MCF10A cells; and when FHIT was knocked down in MCF10A cells the average number of CFS breaks per chromosome was doubled, as in MK−/− cells versus MK+/+ cells.

The CGH array analysis results provide further evidence for increased genome instability in MCF10A FHIT KD cells as copy number alterations in these cells were increased compared with control cells after 30 days of FHIT KD. Parental MCF10A cells exhibit a t(3;9)(pl3;p22) that results in complete loss of the *CDKN2A* and *CDKN2B* loci on chromosome 9 (Soule et al., 1990; Kadota et al., 2010), leading to immortality of the cells, though xenografts of the cells are non-tumorigenic (Worsham et al., 2006). After silencing *FHIT* in MCF10A cells, we observed chromosomal losses or gains at 3p14.2, 7q34, 9q21.3, 15q22.2, 16q23.3, and 3p21.2, which carry tumor suppressor genes or oncogenes, respectively which are associated with cancer development. For example, the *RORA* gene at *FRA15A* (15q22.2), deleted after FHIT KD, is expressed in normal breast, prostate and ovarian epithelium and is frequently inactivated in cancers that arise from these organs (Zhu et al., 2006). Increased

copy number variations and deletion of possible tumor suppressors after FHIT KD support our proposal that FHIT loss leads to genomic instability and contributes to cancer development.

Supplementary Material

Refer to Web version on PubMed Central for supplementary material.

ACKNOWLEDGMENTS

The authors thank Dr. Tsonwin Hai of the Department of Molecular and Cellular Biochemistry at OSU for the MCF10A cells, Dr. Bert Vogelstein of Johns Hopkins University for the HCT116 cells and members of the Huebner lab for helpful discussions. The authors also thank Teresa Druck for MS editing and expert help with preparation of illustrations.

Supported by: US National Institutes of Health, Grant numbers: CA120516, CA154200, and CA132453 (to K.H.); Pelotonia Postdoctoral Fellowship, Ohio State University Comprehensive Cancer Center (to S.A.H.); US National Institutes of Health, Grant numbers: F31CA157150 and T32GM068412 (to J.C.S.); Director, Office of Science, Office of Biological and Environmental Research, of the U.S. Department of Energy, Grant numbers: DE-AC02-05CH11231 (to M.R.S.).

REFERENCES

Bartkova J, Horejsi Z, Koed K, Kramer A, Tort F, Zieger K, Guldberg P, Sehested M, Nesland JM, Lukas C, Bartek J. DNA damage response as a candidate anti-cancer barrier in early human tumorigenesis. Nature. 2005; 434:864–870. [PubMed: 15829956]

Bignell GR, Greenman CD, Davies H, Butler AP, Edkins S, Andrews JM, Buck G, Chen L, Beare D, Latimer C, Widaa S, Hinton J, Fahey C, Fu B, Swamy S, Dalgliesh GL, Teh BT, Deloukas P, Yang F, Campbell PJ, Futreal PA, Stratton MR. Signatures of mutation and selection in the cancer genome. Nature. 2010; 463:893–898. [PubMed: 20164919]

Boberg DR, Batistela MS, Pecharki M, Ribeiro EM, Cavalli IJ, Lima RS, Urban CA, Furtado-Alle L, Souza RL. Copy number variation in ACHE/EPHB4 (7q22) and in BCHE/MME (3q26) genes in sporadic breast cancer. Chem Biol Interact. 2013; 203:344–347. [PubMed: 23063927]

Brown KK, Alkuraya FS, Matos M, Robertson RL, Kimonis VE, Morton CC. NR2F1 deletion in a patient with a de novo paracentric inversion, inv(5)(q15q33.2), and syndromic deafness. Am J Med Genet A. 2009; 149:931–938. [PubMed: 19353646]

Cengiz B, Gunduz M, Nagatsuka H, Beder L, Gunduz E, Tamamura R, Mahmut N, Fukushima K, Ali MA, Naomoto Y, Shimizu K, Nagai N. Fine deletion mapping of chromosome 2q21–37 shows three preferentially deleted regions in oral cancer. Oral Oncol. 2007; 43:241–247. [PubMed: 16857411]

Chien J, Narita K, Rattan R, Giri S, Shridhar R, Staub J, Beleford D, Lai J, Roberts LR, Molina J, Kaufmann SH, Prendergast GC, Shridhar V. A role for candidate tumor-suppressor gene TCEAL7 in the regulation of c-Myc activity, cyclin D1 levels and cellular transformation. Oncogene. 2008; 27:7223–7234. [PubMed: 18806825]

Consortium EP. A user's guide to the encyclopedia of DNA elements (ENCODE). PLoS Biol. 2011; 9:e1001046. [PubMed: 21526222]

Consortium EP. An integrated encyclopedia of DNA elements in the human genome. Nature. 2012; 489:57–74. [PubMed: 22955616]

Debatisse M, Le Tallec B, Letessier A, Dutrillaux B, Brison O. Common fragile sites: Mechanisms of instability revisited. Trends Genet. 2012; 28:22–32. [PubMed: 22094264]

Djalali M, Adolph S, Steinbach P, Winking H, Hameister H. A comparative mapping study of fragile sites in the human and murine genomes. Hum Genet. 1987; 77:157–162. [PubMed: 3653889]

Dohi O, Takada H, Wakabayashi N, Yasui K, Sakakura C, Mitsufuji S, Naito Y, Taniwaki M, Yoshikawa T. Epigenetic silencing of RELN in gastric cancer. Int J Oncol. 2010; 36:85–92. [PubMed: 19956836]

Finch R, Moore HG, Lindor N, Jalal SM, Markowitz A, Suresh J, Offit K, Guillem JG. Familial adenomatous polyposis and mental retardation caused by a de novo chromosomal deletion at 5q15-q22: Report of a case. Dis Colon Rectum. 2005; 48:2148–2152. [PubMed: 16228830]

Gorgoulis VG, Vassiliou LV, Karakaidos P, Zacharatos P, Kotsinas A, Liloglou T, Venere M, Ditullio RA Jr. Kastrinakis NG, Levy B, Kletsas D, Yoneta A, Herlyn M, Kittas C, Halazonetis TD. Activation of the DNA damage checkpoint and genomic instability in human precancerous lesions. Nature. 2005; 434:907–913. [PubMed: 15829965]

Grady B, Goharderakhshan R, Chang J, Ribeiro-Filho LA, Perinchery G, Franks J, Presti J, Carroll P, Dahiya R. Frequently deleted loci on chromosome 9 may harbor several tumor suppressor genes in human renal cell carcinoma. J Urol. 2001; 166:1088–1092. [PubMed: 11490304]

Guler G, Uner A, Guler N, Han SY, Iliopoulos D, Hauck WW, McCue P, Huebner K. The fragile genes FHIT and WWOX are inactivated coordinately in invasive breast carcinoma. Cancer. 2004; 100:1605–1614. [PubMed: 15073846]

Hagmar L, Bonassi S, Stromberg U, Brogger A, Knudsen LE, Norppa H, Reuterwall C. Chromosomal aberrations in lymphocytes predict human cancer: A report from the European Study Group on Cytogenetic Biomarkers and Health (ESCH). Cancer Res. 1998; 58:4117–4121. [PubMed: 9751622]

Hansen RS, Thomas S, Sandstrom R, Canfield TK, Thurman RE, Weaver M, Dorschner MO, Gartler SM, Stamatoyannopoulos JA. Sequencing newly replicated DNA reveals widespread plasticity in human replication timing. Proc Natl Acad Sci USA. 2010; 107:139–144. [PubMed: 19966280]

Huebner K. DNA fragility put into context. Nature. 2011; 470:46–47. [PubMed: 21293366]

Huebner K, Croce CM. FRA3B and other common fragile sites: The weakest links. Nat Rev Cancer. 2001; 1:214–221. [PubMed: 11902576]

Iarmarcovai G, Bonassi S, Botta A, Baan RA, Orsiere T. Genetic polymorphisms and micronucleus formation: A review of the literature. Mutat Res. 2008; 658:215–233. [PubMed: 18037339]

Jongsma AP, Piek JM, Zweemer RP, Verheijen RH, Klein Gebbinck JW, van Kamp GJ, Jacobs IJ, Shaw P, van Diest PJ, Kenemans P. Molecular evidence for putative tumour suppressor genes on chromosome 13q specific to BRCA1 related ovarian and fallopian tube cancer. Mol Pathol. 2002; 55:305–309. [PubMed: 12354934]

Kadota M, Yang HH, Gomez B, Sato M, Clifford RJ, Meerzaman D, Dunn BK, Wakefield LM, Lee MP. Delineating genetic alterations for tumor progression in the MCF10A series of breast cancer cell lines. PLoS One. 2010; 5:e9201. [PubMed: 20169162]

Keller PJ, Arendt LM, Skibinski A, Logvinenko T, Klebba I, Dong S, Smith AE, Prat A, Perou CM, Gilmore H, Schnitt S, Naber SP, Garlick JA, Kuperwasser C. Defining the cellular precursors to human breast cancer. Proc Natl Acad Sci USA. 2012; 109:2772–2777. [PubMed: 21940501]

Kim YH, Lachuer J, Mittelbronn M, Paulus W, Brokinkel B, Keyvani K, Sure U, Wrede K, Nobusawa S, Nakazato Y, Tanaka Y, Vital A, Mariani L, Ohgaki H. Alterations in the RB1 pathway in low-grade diffuse gliomas lacking common genetic alterations. Brain Pathol. 2011; 21:645–651. [PubMed: 21470325]

Kohno T, Otsuka T, Inazawa J, Abe T, Yokota J. Breakpoint junction of interstitial homozygous deletion at chromosome 2q33 in a small cell lung carcinoma. DNA Res. 1996; 3:421–424. [PubMed: 9097045]

Krummel KA, Denison SR, Calhoun E, Phillips LA, Smith DI. The common fragile site FRA16D and its associated gene WWOX are highly conserved in the mouse at Fra8E1. Genes Chromosomes Cancer. 2002; 34:154–167. [PubMed: 11979549]

Lee SH, Shin MS, Kim HS, Park WS, Kim SY, Lee HK, Park JY, Oh RR, Jang JJ, Park KM, Han JY, Kang CS, Lee JY, Yoo NJ. Point mutations and deletions of the Bcl10 gene in solid tumors and malignant lymphomas. Cancer Res. 1999; 59:5674–5677. [PubMed: 10582682]

Letessier A, Millot GA, Koundrioukoff S, Lachages AM, Vogt N, Hansen RS, Malfoy B, Brison O, Debatisse M. Cell-type-specific replication initiation programs set fragility of the FRA3B fragile site. Nature. 2011; 470:120–123. [PubMed: 21258320]

Mori M, Mimori K, Shiraishi T, Alder H, Inoue H, Tanaka Y, Sugimachi K, Huebner K, Croce CM. Altered expression of Fhit in carcinoma and precarcinomatous lesions of the esophagus. Cancer Res. 2000; 60:1177–1182. [PubMed: 10728669]

Mrasek K, Schoder C, Teichmann AC, Behr K, Franze B, Wilhelm K, Blaurock N, Claussen U, Liehr T, Weise A. Global screening and extended nomenclature for 230 aphidicolin-inducible fragile sites, including 61 yet unreported ones. Int J Oncol. 2010; 36:929–940. [PubMed: 20198338]

Murano I, Kuwano A, Kajii T. Cell type-dependent difference in the distribution and frequency of aphidicolin-induced fragile sites: T and B lymphocytes and bone marrow cells. Hum Genet. 1989a; 84:71–74. [PubMed: 2514134]

Murano I, Kuwano A, Kajii T. Fibroblast-specific common fragile sites induced by aphidicolin. Hum Genet. 1989b; 83:45–48. [PubMed: 2504659]

Negrini S, Gorgoulis VG, Halazonetis TD. Genomic instability–An evolving hallmark of cancer. Nat Rev Mol Cell Biol. 2010; 11:220–228. [PubMed: 20177397]

Ohta M, Inoue H, Cotticelli MG, Kastury K, Baffa R, Palazzo J, Siprashvili Z, Mori M, McCue P, Druck T, Croce CM, Huebner K. The FHIT gene, spanning the chromosome 3p14.2 fragile site and renal carcinoma-associated t(3;8) breakpoint, is abnormal in digestive tract cancers. Cell. 1996; 84:587–597. [PubMed: 8598045]

Ozeri-Galai E, Bester AC, Kerem B. The complex basis underlying common fragile site instability in cancer. Trends Genet. 2012; 28:295–302. [PubMed: 22465609]

Paddison PJ, Caudy AA, Bernstein E, Hannon GJ, Conklin DS. Short hairpin RNAs (shRNAs) induce sequence-specific silencing in mammalian cells. Genes Dev. 2002; 16:948–958. [PubMed: 11959843]

Rao PH, Arias-Pulido H, Lu XY, Harris CP, Vargas H, Zhang FF, Narayan G, Schneider A, Terry MB, Murty VV. Chromosomal amplifications, 3q gain and deletions of 2q33-q37 are the frequent genetic changes in cervical carcinoma. BMC Cancer. 2004; 4:5. [PubMed: 15018632]

Rothenberg SM, Mohapatra G, Rivera MN, Winokur D, Greninger P, Nitta M, Sadow PM, Sooriyakumar G, Brannigan BW, Ulman MJ, Perera RM, Wang R, Tam A, Ma XJ, Erlander M, Sgroi DC, Rocco JW, Lingen MW, Cohen EE, Louis DN, Settleman J, Haber DA. A genome-wide screen for microdeletions reveals disruption of polarity complex genes in diverse human cancers. Cancer Res. 2010; 70:2158–2164. [PubMed: 20215515]

Saldivar JC, Miuma S, Bene J, Hosseini SA, Shibata H, Sun J, Wheeler LJ, Mathews CK, Huebner K. Initiation of genome instability and preneoplastic processes through loss of Fhit expression. PLoS Genet. 2012; 8:e1003077. [PubMed: 23209436]

Seabright M. A rapid banding technique for human chromosomes. Lancet. 1971; 2:971–972. [PubMed: 4107917]

Simoneau M, LaRue H, Aboulkassim TO, Meyer F, Moore L, Fradet Y. Chromosome 9 deletions and recurrence of superficial bladder cancer: Identification of four regions of prognostic interest. Oncogene. 2000; 19:6317–6323. [PubMed: 11175346]

Sonoda E, Sasaki MS, Morrison C, Yamaguchi-Iwai Y, Takata M, Takeda S. Sister chromatid exchanges are mediated by homologous recombination in vertebrate cells. Mol Cell Biol. 1999; 19:5166–5169. [PubMed: 10373565]

Soule HD, Maloney TM, Wolman SR, Peterson WD Jr. Brenz R, McGrath CM, Russo J, Pauley RJ, Jones RF, Brooks SC. Isolation and characterization of a spontaneously immortalized human breast epithelial cell line, MCF-10. Cancer Res. 1990; 50:6075–6086. [PubMed: 1975513]

Sozzi G, Pastorino U, Moiraghi L, Tagliabue E, Pezzella F, Ghirelli C, Tornielli S, Sard L, Huebner K, Pierotti MA, Croce CM, Pilotti S. Loss of FHIT function in lung cancer and preinvasive bronchial lesions. Cancer Res. 1998; 58:5032–5037. [PubMed: 9823304]

Stampfer MR, Bartley JC. Induction of transformation and continuous cell lines from normal human mammary epithelial cells after exposure to benzo[a]pyrene. Proc Natl Acad Sci USA. 1985; 82:2394–2398. [PubMed: 3857588]

Stankov K, Pastore A, Toschi L, McKay J, Lesueur F, Kraimps JL, Bonneau D, Gibelin H, Levillain P, Volante M, Papotti M, Romeo G. Allelic loss on chromosomes 2q21 and 19p 13.2 in oxyphilic thyroid tumors. Int J Cancer. 2004; 111:463–467. [PubMed: 15221978]

Turner BC, Ottey M, Zimonjic DB, Potoczek M, Hauck WW, Pequignot E, Keck-Waggoner CL, Sevignani C, Aldaz CM, McCue PA, Palazzo J, Huebner K, Popescu NC. The fragile histidine triad/common chromosome fragile site 3B locus and repair-deficient cancers. Cancer Res. 2002; 62:4054–4060. [PubMed: 12124341]

Wistuba, Behrens C, Virmani AK, Mele G, Milchgrub S, Girard L, Fondon JW III, Garner HR, McKay B, Latif F, Lerman MI, Lam S, Gazdar AF, Minna JD. High resolution chromosome 3p allelotyping of human lung cancer and preneoplastic/preinvasive bronchial epithelium reveals multiple, discontinuous sites of 3p allele loss and three regions of frequent breakpoints. Cancer Res. 2000; 60:1949–1960. [PubMed: 10766185]

Worsham MJ, Benninger MJ, Zarbo RJ, Carey TE, Van Dyke DL. Deletion 9p22-pter and loss of Y as primary chromosome abnormalities in a squamous cell carcinoma of the vocal cord. Genes Chromosomes Cancer. 1993; 6:58–60. [PubMed: 7680223]

Worsham MJ, Pals G, Schouten JP, Miller F, Tiwari N, van Spaendonk R, Wolman SR. High-resolution mapping of molecular events associated with immortalization, transformation, and progression to breast cancer in the MCF10 model. Breast Cancer Res Treat. 2006; 96:177–186. [PubMed: 16319984]

Zhu Y, McAvoy S, Kuhn R, Smith DI. RORA, a large common fragile site gene, is involved in cellular stress response. Oncogene. 2006; 25:2901–2908. [PubMed: 16462772]

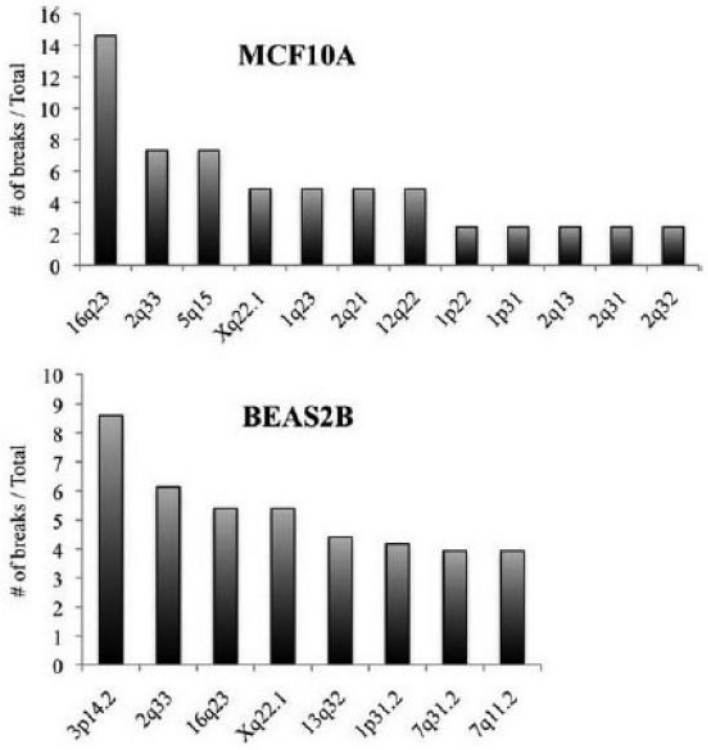

Figure 1.

CFSs in human epithelia-derived cells. Upper panel, frequency of Aph-induced breaks at individual CFSs in MCF10A breast epithelial cells; the 16q23/*WWOX* locus is most frequently expressed in MCF10A cells. Lower panel, expression of CFSs in BEAS2B cells; note that the *FRA3B*/*FHIT* locus at 3p14.2 is the most fragile locus in these SV40 T immortalized lung epithelia-derived cells. Otherwise the range of fragile sites is similar to those in MCF10A.

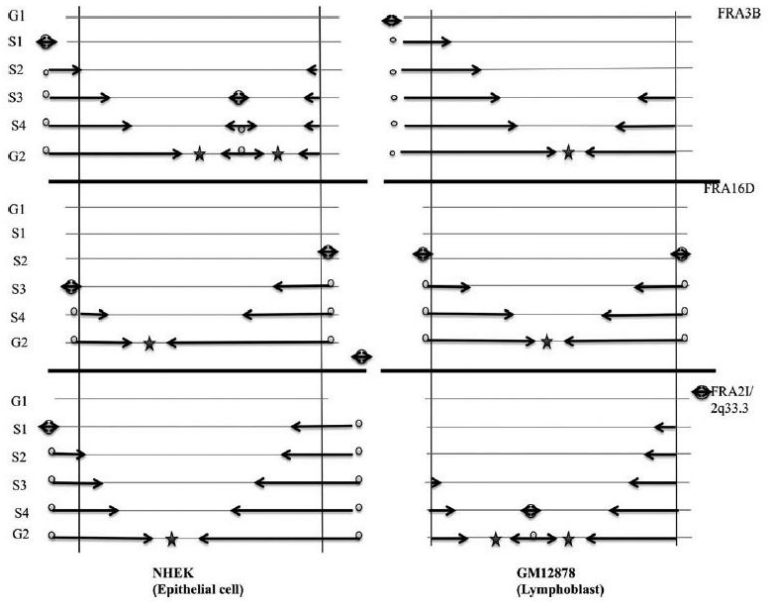

Figure 2.

Repli-seq data for *FRA3B*, *FRA16D*, and *FRA2I* in human epithelial and lymphoblast cells. Drawings representative of replication dynamics in the core regions of *FRA3B*/3p14.2, *FRA16D*/16q23.3, and *FRA2I*/2q33.3 from ENCODE Repli-Seq database: Right panel. Human lymphoblast cell; core regions are delimitated by vertical lines and cell cycle phases are indicated on the left with S phase subdivided into four fractions; the cores are poor in initiation events in most lymphoblasts for *FRA3B* and *FRA16D* and during unperturbed S phase are replicated by long-traveling forks emanating from origins located in the flanking regions that fire around early or mid-S phase. Convergent forks merge in G2 phase, resulting in late completion of the core replication. At *FRA2I*/2q33.3, encompassing the *PARD3B* gene, lymphoblasts show one replication origin at the end of S phase, possibly accounting for a low frequency of CFS activity at 2q33.3 in lymphoblasts compared with *FRA3B* and *FRA16D*. Repli-Seq data have been used from Replication Timing by Repli-seq from ENCODE/University of Washington database according to the ENCODE data release policy (Consortium, 2011, 2012). Left panel depicts the core regions for the same loci, *FRA3B*, *FRA16D*, and *FRA2I*, in the epithelial cell line, NHEK.

Passage 8	# of Meta-phases	# of Chromo-somes	Breaks/ Chromosome	% diploid	% tetraploid	% aneuploid
Fhit$^{+/+}$	70	3340	0.008	78.6	15.7	5.7
Fhit$^{-/-}$	75	4268	0.016	54.7	14.7	30.7
Fhit$^{+/+}$ (Aph)	90	4268	0.046			
Fhit$^{-/-}$ (Aph)	90	5144	0.087			

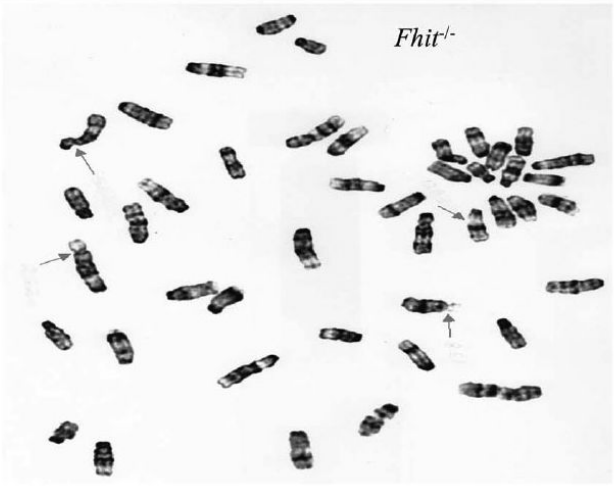

Figure 3.

Spontaneous and Aph-induced breaks in *Fhit*+/+ and *Fhit*−/− MK cells. Upper panel. Mean overall spontaneous chromosome gaps and breaks per chromosome in *Fhit*+/+ (WT) and *Fhit*−/− MK cells. There is an approximately twofold increase in breaks per chromosome in *Fhit*−/− MK cells compared with the *Fhit*+/+ cells and an increase in % aneuploidy and tetraploidy in *Fhit*−/− MK cells relative to the *Fhit*+/+ cells. Cells were subcultured eight times and metaphase chromosomes prepared and counted (*n* 5 70 for *Fhit*+/+; *n* 5 75 for *Fhit* −/− metaphases). Lower panel. Representative breaks on Giemsa-stained metaphase of *Fhit* −/− cells treated with 0.4 lM Aph for 18 hr. Arrows indicate chromosome breaks.

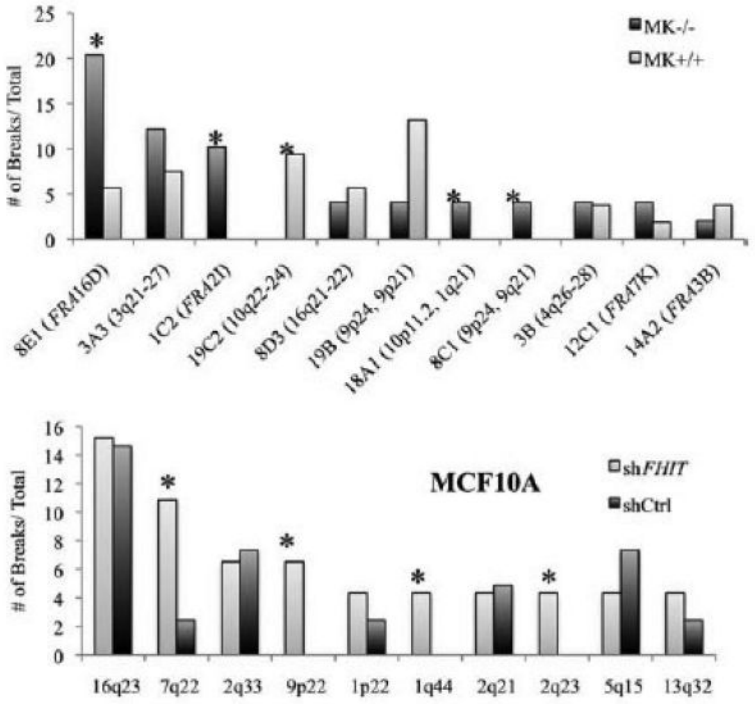

Figure 4.

CFSs in epithelial cells with and without FHIT protein expression. Upper panel, comparison of frequencies of Aph-induced breaks at individual CFSs in the *Fhit*−/− and *Fhit*+/+ MK cells. Asterisks note fragile sites that vary extensively in frequency in the cells with absence of Fhit expression. The human homologous region for each mouse CFS is noted in parentheses. Lower panel, a similar comparison of numbers of breaks at CFSs in MCF10A cells infected with shCtrl or sh*FHIT* lentivirus vectors; the order of frequency of the most fragile loci varies slightly in the two cell types, but the 16q23/*WWOX* locus remains the most frequently expressed in both cell lines.

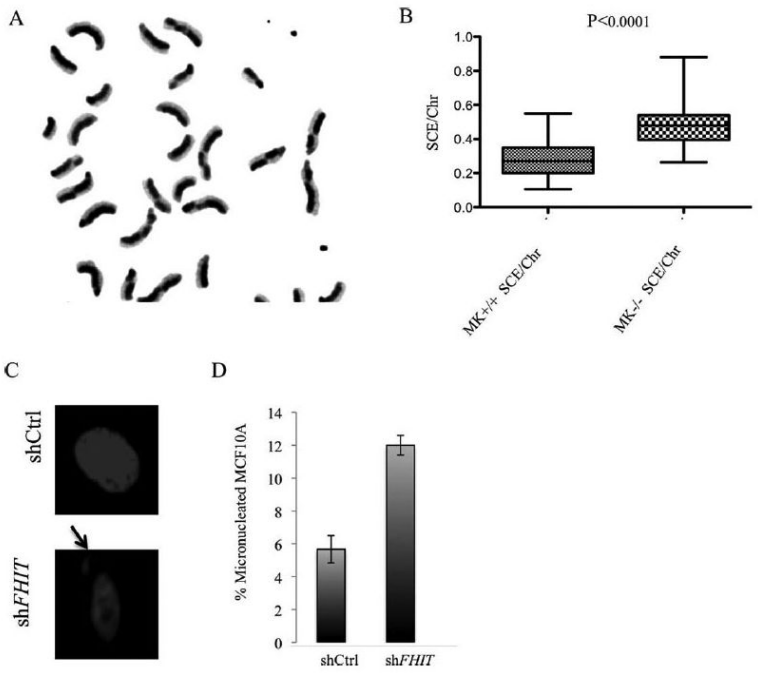

Figure 5.

Sister chromatid exchange in mouse kidney cells. (A) *Fhit*−/− MK metaphase illustrating differential staining of sister chromatids and sites of sister-chromatid exchange (SCE). (B) SCE frequency is increased in *Fhit*−/− cells relative to *Fhit*+/+ cells. Statistical significance was assessed using two-sided student's *t*-test. (C) Effect of FHIT knockdown on development of micronuclei in MCF10A cells. Representative images of DAPI-stained nuclei in shCtrl and sh*FHIT* cells are shown. Arrow marks a micronucleus. (D) Quantification of micronucleated cells 7 days after shRNA transfections in MCF10A cells. Bar graphs represent the means, and error bars mark the standard deviations. *P* values determined using a two-sided *t*-test ($P < 0.005$).

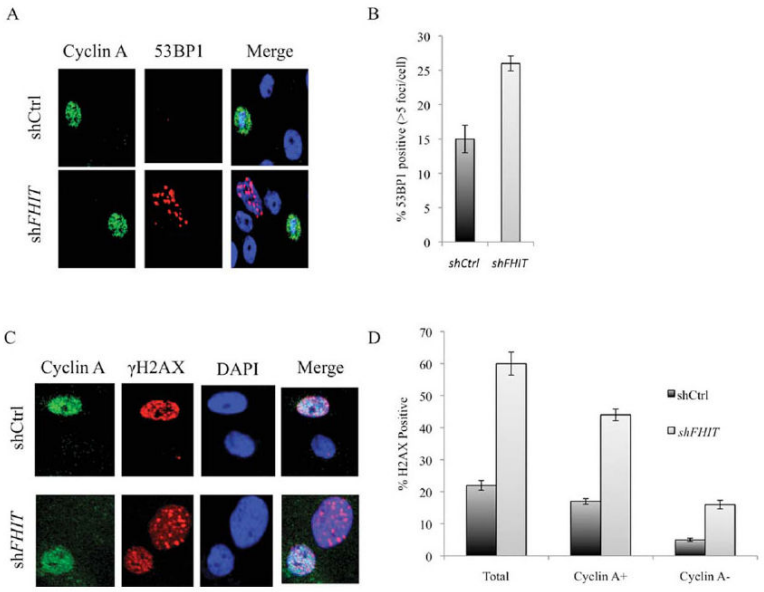

Figure 6.

γH2AX foci and 53BP1 bodies in FHIT-deficient MCF10A cells. (A) Immunofluorescent detection of Cyclin A and 53BP1 in MCF10A cells after FHIT knockdown. Cyclin A-positive cells identify S phase cells and establish that the 53BP1 bodies are mostly in G1 cells. Representative images are shown. (B) Histograms of 53BP1 nuclear bodies/G1 phase cell 7 days following shRNA transfection. Data obtained were quantified from three independent experiments and statistical significance determined using a two-sided *t*-test. Bar graphs represent the means, and error bars mark the standard deviation. The data show that there is a significant association of level of 53BP1 bodies with FHIT-deficiency in MCF10A cells ($P < 0.05$). (C) Coimmunostaining of MCF10A cells for Cyclin A and γH2AX. (D) Histograms of γH2AX foci show a significant increase in numbers of γH2AX foci in FHIT KD cells compared with FHIT-expressing cells.

TABLE 1

CFSs in Order of High to Low Frequency in Epithelial Cells Versus Lymphoblasts and Fibroblasts

MCF10A	MCF10A *FHIT* KD	184A1	HCT116	BEAS-2B	GM1500	Lympho blasts (Mrasek et al., 2010)	MRC-5 fibroblasts (Letessier et al., 2011)	Primary Fibroblasts (Murano et al., 1989b)
16q23	16q23	16q23	16q23	3p14.2	16q23	3p14.2	3q13.3	3q26.2
2q33	7q22	3q26.2	2q33	2q33	3p14.2	16q23.2	1p31.1	7q11.2
5q15	2q33	Xq22.1	4q21.3	16q23	4q35	Xp22.3	16q23	16q23
Xq22.1	9p22	12q22	Xp22.3	Xq22.1	8q22	2q32.1	2q22	1p31
1q23	5q15	14q24.3	Xq22.1	13q32	Xp22.1	1p21.3	3q28	10q11.2
2q21	Xq22.1	7q11.2	7q31.2	1p31.2	6q25.1	6q26	3q12	12q23
12q22	2q21	Xp21.2	3q25	7q31.2	1p22	7q31.1	7q31.1	7q31
1p22	1p22	13q14.3	4p15.2	7q11.2	9q12	7q32.2	7q11.2	
1p31	1q44	1p31.2	3p13	22q13	2q22	1q44	3p14.2	
2q13	2q23	13q22	Xp21.2	1p22	3p25	4q31.1	13q31	
0.025	0.058	0.143	0.062	0.139	0.04			

Numbers of metaphases analyzed for CFS enumeration in MCF10A, MCF10A *FHIT* KD, 184A1, HCT116, BEAS2B, and GM1500 is 36, 20, 20, 20, 44, and 20, respectively. Bold numbers in the last row indicate the average number of breaks per chromosome in the epithelial cells versus the lymphoblastoid GM1500 cells.

TABLE 2

Copy Number Alterations Induced by *FHIT* Knockdown in MCF10A Cells

Chromosome	Position on chromosome	Fold change	Cytoband	Representative genes altered
Loss				
3	61002345–61080836	−0.62	p14.2	*FHIT*
7	141750430–141785258	−2.58	q34	*MGAM*
9	21817082–21885202	−4.93	p21.3	*C9orf53*
12	122634121–133779076	−1.72	q24.31–q24.33	*NCOR2*
15	60687251–61144210	−0.74	q22.2	*RORA*
16	83721255–84451167	−0.38	q23.3–q24.1	*CDH13, ADAD2, WFDC1*
22	32092559–32239249	−0.85	q12.2–q12.3	*DEPDC5*
X	1770348–36331235	−0.41	p22.33–p21.1	*ZBED1, CD99*
Gain				
3	51929623–51941665	1.29	p21.2	*IQCF1*
9	137332375–137332434	1.35	q34.2	*RXRA*
10	38240258–38240317	1.31	p11.1	*ZNF25*
11	35269915–35276999	1.43	p13	*SLC1A2*
11	66006136–134927114	0.49	q13.2–q25	*PACS1, RAB1B, CD248, RIN1, B3GNT1, CTSF, SLC29A2*
X	116707254–155232214	0.297	q24–q28	*VAMP7, KLHL13, WDR44*

Fold change: ~−0.5 indicates hemizygous deletion ~−1 homozygous deletion; ~1.5, three copies gained, ~1.0, 2 copies gained, ~0.5, one copy gained. These FHIT loss-induced CNVs are in addition to those that had already occurred in the parental MCF10A and have been described previously (Soule et al., 1990; Worsham et al., 2006; Kadota et al., 2010).

TABLE 3

Candidate Cancer-Relevant Genes Near Epithelial CFS Loci

CFSs	Putative tumor suppressor genes	Cancer cell lines	Reference
1p22	*BCL10*	Breast, colon	Lee et al., 1999
2q21	*R3HDM, LCT, LRP1B*	Oral	Stankov et al., 2004; Cengiz et al., 2007
2q33	*PARD3B, PLCL2*	Lung, breast, glioblastoma	Kohno et al., 1996; Rao et al., 2004; Rothenberg et al., 2010
5q15	*POU5F2, KIAA0825, ANKRD32, MCTP1*	H209 (Lung), HEC-1 uterus, KYSE-30 esoph	Finch et al., 2005; Brown et al., 2009; Rothenberg et al., 2010
7q22	*COL1A2, PRKAR2B, PSMC2, PIK3CG, DLX5, DLX6, PCOLCE, PMS2P1, SERPINE1, TRIP6, CUX1, ORC5, LHFPL3, RELN*	Breast, uterine, gastric	Dohi et al., 2010; Mrasek et al., 2010; Boberg et al., 2012
9p22		Kidney, oral, bladder	Worsham et al., 1993; Simoneau et al., 2000; Grady et al., 2001
13q32	*FARP1, STK24*	NSCLC (VMRC-LCD, H1975), ESSC (CNV)	Jongsma et al., 2002; Rothenberg et al., 2010; Kim et al., 2011
Xq22.1	*TCEAL7*	Ovarian, breast, lung	Chien et al., 2008

Though these new epithelial cell-associated CFSs have not been precisely mapped within the given chromosome bands, the individual chromosome bands harbor genes, listed in column two, that might be near or within the fragile regions. Column three lists types of epithelial cancer-derived cells that exhibit alterations at the specific chromosome bands as reported in the references listed in column 4.